Calcium Phosphate with a Channel-like Morphology by Polymer Templating

Andriy Shkilnyy,[†,‡] Jessica Brandt,[‡] Alexandre Mantion,[§,||] Oskar Paris,[‡,⊥] Helmut Schlaad,[‡] and Andreas Taubert*[,†,‡,§]

Institute of Chemistry, University of Potsdam, Karl-Liebknecht-Str. 24-25, D-14476 Golm, Germany, Max Planck Institute of Colloids and Interfaces, Research Campus Golm, D-14424 Potsdam, Germany, and Department of Chemistry, University of Basel, Klingelbergstr. 80, CH-4056 Basel, Switzerland

Received December 2, 2008. Revised Manuscript Received February 16, 2009

Calcium phosphate mineralization from aqueous solution in the presence of organic growth modifiers has been intensely studied in the recent past. This is mostly due to potential applications of the resulting composites in the biomaterials field. Polymers in particular are efficient growth modifiers. As a result, there has been a large amount of work on polymeric growth modifiers. Interestingly, however, relatively little work has been done on polycationic additives. The current paper shows that poly(ethylene oxide)-*b*-poly(L-lysine) block copolymers lead to an interesting morphology of calcium phosphate precipitated at room temperature and subjected to a mild heat treatment at 85 °C. Electron microscopy, synchrotron X-ray diffraction, and porosity analysis show that a (somewhat) porous material with channel-like features forms. Closer inspection using transmission electron microscopy shows that the channels are probably not real channels. Much rather the morphology is the result of the aggregation of ca. 100-nm-sized rod-like primary particles, which changes upon drying to exhibit the observed channel-like features. Comparison experiments conducted in the absence of polymer and with poly(ethylene oxide)-*b*-poly(L-glutamate) show that these features only form in the presence of the polycationic poly(L-lysine) block, suggesting a distinct interaction of the polycation with either the crystal or the phosphate ions prior to mineralization.

Introduction

Calcium phosphate has been studied extensively as a biomimetic and biocompatible material for many applications, including bone substitutes and drug delivery.[1−7] In particular, the growth of calcium phosphate from aqueous solution in the presence of organic growth modifiers has attracted interest due to its biomimetic twist. Polymers, polymer gels, polymer surfaces, and polymer capsules have been used for the fabrication of a wide variety of composite materials.[8,9] Many studies show that polyelectrolytes are particularly effective growth modifiers for calcium phosphate growth from aqueous solution.[10−16]

Amino acids and poly(amino acids) are also efficient growth modifiers.[8,17−20] The mineralization community has studied both poly(amino acid) homopolymers and block copolymers.[8] For example, glutamic acid (single letter code E), aspartic acid (D), and poly(aspartic acid) strongly affect calcium phosphate mineralization in aqueous solution.[17,18,20] Kakizawa and Kataoka reported the formation of uniform composite nanoparticles by mixing calcium/DNA and phosphate/poly(ethylene oxide) (PEO)-*block*-poly(D) solutions.[3,4]

However, while there has been some work on *anionic* PEO-*b*-poly(amino acid) block copolymers,[8] there have been no calcium phosphate mineralization studies with cationic PEO-*b*-poly(amino acid) block copolymers. This is in line with the general observation that there are only few reports on calcium phosphate mineralization with polycations at all.[13,16,21−23] Similarly, there are only a few studies of the

* Corresponding author: Tel.: ++49 (0)331 977 5773. E-mail: ataubert@uni-potsdam.de.
[†] University of Potsdam.
[‡] Max Planck Institute of Colloids and Interfaces.
[§] University of Basel.
[||] Present address: Federal Institute for Materials Research and Testing (BAM), Richard-Willstätter-Str. 11, 12489 Berlin, Germany.
[⊥] Present address: Institute of Physics, University of Leoben, Franz-Josef-Str. 18, 8700 Leoben, Austria.

(1) Bohner, M.; Gbureck, U.; Barralet, J. E. *Biomaterials* **2005**, *26*, 6423.
(2) Bohner, M. *Injury* **2000**, *31*, 37.
(3) Kakizawa, Y.; Kataoka, K. *Langmuir* **2002**, *18*, 4539.
(4) Kakizawa, Y.; Miyata, K.; Furukawa, S.; Kataoka, K. *Adv. Mater.* **2004**, *16*, 699.
(5) Sokolova, V.; Radtke, I.; Heumann, R.; Epple, M. *Biomaterials* **2006**, *27*, 3147.
(6) Welzel, T.; Radtke, I.; Meyer-Zaika, W.; Heumann, R.; Epple, M. *J. Mater. Chem.* **2004**, *14*, 2213.
(7) Sokolova, V.; Prymak, O.; Meyer-Zaika, W.; Cölfen, H.; Rehage, H.; Shukla, A.; Epple, M. *Materialwiss. Werkstofftech.* **2006**, *37*, 441.
(8) Schweizer, S.; Taubert, A. *Macromol. Biosci.* **2007**, *7*, 1085.
(9) Taubert, A.; Furrer, E.; Meier, W. *Chem. Commun.* **2004**, 2170.
(10) Bertoni, E.; Bigi, A.; Falini, G.; Panzavolta, S.; Roveri, N. *J. Mater. Chem.* **1999**, *9*, 779.
(11) Bigi, A.; Boanini, E.; Borghi, M.; Cojazzi, G.; Panzavolta, S.; Roveri, N. *J. Inorg. Biochem.* **1999**, *75*, 145.
(12) Bigi, A.; Boanini, E.; Walsh, D.; Mann, S. *Angew. Chem., Int. Ed.* **2002**, *41*, 2163.
(13) Michel, M.; Arntz, Y.; Fleith, G.; Toquant, J.; Haikel, Y.; Voegel, J.-C.; Schaaf, P.; Ball, V. *Langmuir* **2006**, *22*, 2358.
(14) Casse, O.; Colombani, O.; Kita-Tockarczyk, K.; Müller, A. H. E.; Meier, W.; Taubert, A. *Faraday Discuss.* **2008**, *139*, 179.
(15) Chen, J.; Chu, B.; Hsiao, B. S. *J. Biomed. Mater. Res., Part A* **2006**, *79A*, 307.
(16) Shkilnyy, A.; Friedrich, A.; Thiersch, B.; Schone, S.; Fechner, M.; Koetz, J.; Schläpfer, C.-W.; Taubert, A. *Langmuir* **2008**, *24*, 2102.
(17) Peytcheva, A.; Cölfen, H.; Schnablegger, H.; Antonietti, M. *Colloid Polym. Sci.* **2002**, *280*, 218.
(18) Bigi, A.; Boanini, E.; Bracci, B.; Falini, G.; Rubini, K. *J. Inorg. Biochem.* **2003**, *95*, 291.

10.1021/cm803244z CCC: $40.75
Published on Web 04/01/2009

interaction of polycations with phosphate ions.[24] These studies have shown that there is in some cases a quite strong effect of polycationic additives on calcium phosphate growth, but there are simply not enough data to accurately determine the role of polycations in the mineralization process. Furthermore, there are no studies on calcium phosphate mineralization with block copolymers with cationic blocks.

We have therefore set out to determine the influence of cationic blocks on calcium phosphate mineralization.[16,25] To enable comparison with earlier studies,[3,4,8,26−29] we have used polymers, where the second block is a PEO block. This paper shows that PEO-*b*-poly(L-lysine) (PEO-*b*-PLK) block copolymers lead to an unexpected morphology of the calcium phosphate precipitate after heat treatment. Comparison experiments conducted in the absence of polymer and with PEO-*b*-poly(L-glutamate) (PEO-*b*-PLE) show that the resulting structure is due to the PEO-*b*-PLK additive and cannot be replicated with a polyanion.

Experimental Part

Materials. All chemicals (analytical grade or chemically pure grade) were purchased from Fluka and Aldrich. The amino-endfunctionalized PEO (PEO-NH_2, number-average molecular weight M_n = 4900 g/mol; polydispersity index PDI = 1.08) was purchased from Rapp Polymere (Tübingen, Germany). PEO-*b*-PLE(Bzl) and PEO-*b*-PLK(Z) were prepared by ring-opening polymerization of the corresponding protected amino acid-*N*-carboxyanhydride using PEO-NH_2 as the macroinitiator, as described elsewhere.[30−32] Mole fractions of PLE(Bzl) and PLK(Z) were 0.21 and 0.20, respectively (^{1}H NMR); PDIs of the block copolymers were 1.26 and 1.30, respectively (size exclusion chromatography, SEC; Figure S5, Supporting Information). Protecting groups were quantitatively removed by alkaline (Bzl) or acidic hydrolysis (Z), as confirmed by ^{1}H NMR (Figure S5, Supporting Information).

Mineralization. Mineralization was done as described previously.[16] Polymer concentrations were varied from 8 to 12 mg/mL. In a typical synthesis, 4 mL of a polymer-containing 0.48 M $CaCl_2$ solution were mixed with 4 mL of a polymer-containing 0.24 M $(NH_4)_2HPO_4$ solution. Upon mixing, the solution immediately became milky. Directly after mixing, the pH was adjusted to 5 or 8 using 1 M KOH. Thereafter, the mixtures were gently agitated at 36.6 °C using a Unihood 550 system. After seven days, the precipitates were centrifuged, washed with THF, and dried for one day at room temperature. The powders were annealed for 4 days at 85 °C. Additional mineralization experiments were performed in 50/50 (v/v) methanol/water mixtures. Five milliliters of a 0.24 M phosphoric acid solution in methanol was added to a 0.48 M $CaCl_2$ solution in water.

Characterization. X-ray powder diffraction was done on a Nonius PDS 120 with Cu Kα radiation and position sensitive detector and on a Nonius D8 with Cu Kα radiation. Analysis of the XRD patterns was done with OriginLab Origin 6.1. Synchrotron microcrystal diffraction was performed at the μ-Spot beamline at BESSY II (Berlin, Germany).[33,34] The beam was monochromatized with a Si 111 double crystal monochromator (wavelength λ = 0.0688 nm) and focused to a spot of 50 μm at the sample position using a toroidal mirror and a beam-defining pinhole. Data were collected using a CCD based area detector (MarMosaic 225, MarUSA, Evanston). Transmission infrared (IR) spectra were recorded on a Thermo Nicolet Nexus 670 FTIR spectrometer. Samples were ground with KBr and pressed into pellets using a hand press. Spectra were recorded at room temperature from 400 to 4000 cm^{-1} with a resolution of 4 cm^{-1}. Scanning electron microscopy experiments were done on a Hitachi S-4800 operated at 5 kV. Prior to imaging, samples were sputtered with Pt/Au using a Balzers SCD 050 Sputter Coater. Transmission electron microscopy was done on a Zeiss 912 Omega operated at 120 kV. Cross sections were obtained with a Leica Ultra Cut Microtome. For sectioning, the powder samples were embedded in "LR white" resin (Plano GmbH). Samples were cut at 1 mm/s at room temperature. Raman spectra were acquired using a CRM200 confocal Raman microscope (WITEC, Germany) with a Nikon objective (10×, NA = 0.25) and a linearly polarized laser (diode pumped green laser, λ = 532 nm, CrystaLaser). Thermogravimetric analysis and differential thermal analysis was done on a Linseis L81 thermal analyzer. Samples were heated in air at 10 °C/min from 30 to 1000 °C. BET measurements were performed on a Micromeritics Tristar 3000 automated gas adsorption analyzer. Prior to analysis, the samples were degassed in a Micromeritics VacPrep061 degasser overnight at 150 °C and under 100 μTorr pressure.

Results

Calcium phosphate was grown in the absence of polymer and in the presence of PEO-*b*-PLK and PEO-*b*-PLE using a procedure published earlier.[16] X-ray diffraction (XRD) shows that the initial pH of the reaction mixture is the key responsible for the selection of the crystal phase, consistent with earlier studies.[16,35−37] Control samples precipitated in the absence of polymer are, like in our earlier report,[16] pure brushite (dicalcium phosphate dihydrate, DCPD) if precipitated from solutions with an initial pH 5 and pure hydroxyapatite (HAP) if precipitated from solutions with an initial pH 8 (see Supporting Information, Figure S1). Similarly, mineralization in the presence of polymers at an initial pH

(19) Bigi, A.; Boanini, E.; Gazzano, M.; Kojdecki, M. A.; Rubini, K. *J. Mater. Chem.* **2004**, *14*, 274.
(20) Boanini, E.; Torricelli, P.; Gazzano, M.; Giardino, R.; Bigi, A. *Biomaterials* **2006**, *27*, 4428.
(21) Crowther, R. C.; Pritchard, C. M.; Qiu, S. M.; Soloway, R. D. *Liver* **1993**, *13*, 141.
(22) Ngankam, P. A.; Lavalle, P.; Voegel, J. C.; Szyk, L.; Decher, G.; Schaaf, P.; Cuisinier, F. J. G. *J. Am. Chem. Soc.* **2000**, *122*, 8998.
(23) Ball, V.; Michel, M.; Boulmedais, F.; Hemmerle, J.; Haikel, Y.; Schaaf, P.; Voegel, J. C. *Cryst. Growth Des.* **2006**, *6*, 327.
(24) Lutz, K.; Groeger, C.; Sumper, M.; Brunner, E. *Phys. Chem. Chem. Phys.* **2005**, *7*, 2812.
(25) Shkilnyy, A.; Gräf, R.; Hiebl, B.; Neffe, A. T.; Friedrich, A.; Hartmann, J.; Taubert, A. *Macromol. Biosci* **2009**, *9*, 179.
(26) Peytcheva, A.; Cölfen, H.; Schnablegger, H.; Antonietti, M. *Colloid Polym. Sci.* **2002**, *280*, 218.
(27) Bigi, A.; Boanini, E.; Bracci, B.; Falini, G.; Rubini, K. *J. Inorg. Biochem.* **2003**, *95*, 291.
(28) Bigi, A.; Boanini, E.; Gazzano, M.; Kojdecki, M. A.; Rubini, K. *J. Mater. Chem.* **2004**, *14*, 174.
(29) Boanini, E.; Torricelli, P.; Gazzano, M.; Giardino, R.; Bigi, A. *Biomaterials* **2006**, *27*, 4428.
(30) Yotzoyama, M.; Inue, S.; Kataoka, K.; Yui, N.; Sakurai, Y. *Macromol. Rapid. Commun.* **1987**, *8*, 431.
(31) Cornille, F.; Copier, J.-L.; Senet, J.-P. United States Patent 6479665, 2002.
(32) Dimitrov, I.; Kukula, H.; Cölfen, H.; Schlaad, H. *Macromol. Symp.* **2004**, *215*, 383.
(33) Paris, O.; Li, C.; Siegel, S.; Weseloh, G.; Emmerling, F.; Riesemeier, H.; Erko, A.; Fratzl, P. *J. Appl. Crystallogr.* **2007**, *40*, s466.
(34) Paris, O. *Biointerphases* **2008**, *3*, FB16.
(35) Salahi, E.; Moztarzadeh, F. *Ceram. Forum Int.* **2001**, *78*, E43.
(36) Ferraz, M. P.; Monteiro, J.; Manuel, C. M. *J. Appl. Biomater. Biomech.* **2004**, *2*, 74.
(37) Honda, Y.; Kamakura, S.; Sasaki, K.; Suzuki, O. *J. Biomed. Mater. Res. B* **2007**, *80*, 281.

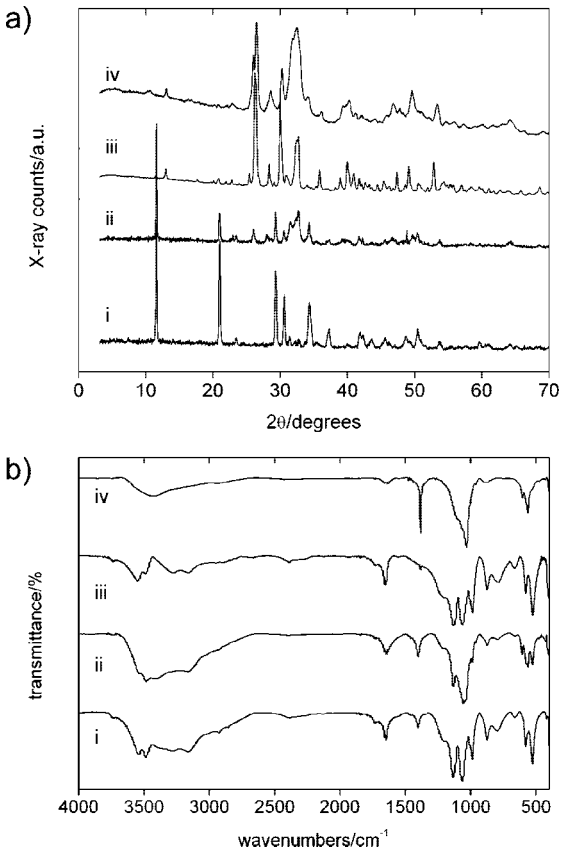

Figure 1. (a) Representative X-ray patterns and (b) IR spectra of precipitates obtained from solutions at an initial pH 5. (i) Brushite, sample precipitated with 8 mg/mL of PEO-*b*-PLE, (ii) brushite/HAP, sample precipitated with 8 mg/mL of PEO-*b*-PLK, (iii) monetite, sample precipitated with 8 mg/mL of PEO-*b*-PLE after annealing at 85 °C for 4 days, (iv) monetite/HAP, sample precipitated with 8 mg/mL of PEO-*b*-PLK after annealing at 85 °C for 4 days.

8 exclusively yields HAP nanoparticles (Supporting Information, Figure S2).

Figure 1 shows representative IR spectra and powder XRD patterns of some precipitates grown with PEO-*b*-PLK and PEO-*b*-PLE starting from solutions with an initial pH 5. XRD shows that in both cases, the main crystal phase is brushite, but there are significant differences between the polymers. For samples grown with PEO-*b*-PLE, Rietveld refinement yields a composition of 98% brushite and 2% HAP. For samples grown with PEO-*b*-PLK, Rietveld refinement was not possible because of too broad HAP lines between 30 and 35° 2θ, but estimates from the reflection intensities indicate a composition of about 60% brushite and 40% HAP. This finding suggests that the pK_a values of the polymers have a quite dramatic influence on the mineralization process. While the anionic PEO-*b*-PLE (p$K_a \sim 5$) almost exclusively leads to the low pH modification brushite, the presence of the cationic PEO-*b*-PLK (p$K_a \sim 10$) leads to a significant fraction of the high pH modification HAP.[38] Although the overall solution pH is roughly the same, these findings suggest that there could be microscopic regions, where the pH is higher in the case of PEO-*b*-PLK, and therefore, a significant fraction of HAP forms.

Figure 1 also shows that annealing at 85 °C induces a phase transition, but again there are differences between the different polymers. For samples grown with PEO-*b*-PLE, Rietveld refinement yields a composition of 94% of monetite (dicalcium phosphate anhydrous, DCPA, a water-free relative of brushite), 5.5% of HAP, and 0.5% of brushite. Again, Rietveld refinement was not possible for samples grown with PEO-*b*-PLK, but estimates from the reflection intensities suggest a composition of about 45% monetite and 55% HAP. In summary, XRD shows that there is, expectedly, a heat-induced dehydration from brushite ($CaHPO_4 \times 2H_2O$) to monetite ($CaHPO_4$) in all samples. However, samples precipitated with PEO-*b*-PLK (from solutions with pH 5!) also contain a significant amount of HAP, which does not change during the annealing process.

IR spectroscopy confirms the XRD structure assignments. IR spectra of the as-prepared phosphates have a broad band between 3700 and 2500 cm^{-1}, which is assigned to stretching modes of hydrogen-bonded crystal water and the hydroxyl group of hydrogen phosphate. Upon annealing at 85 °C, these bands are drastically reduced due to desorption of water. The shoulder at 1250 to 1190 cm^{-1} is attributed to in-plane bending modes of interphosphate or water-to-orthophosphate hydrogen bonds.[39]

Furthermore, all IR spectra exhibit bands that are characteristic of the tetrahedral PO_4 unit.[40,41] The spectra of brushite samples prepared from solutions at an initial pH 5 exhibit bands at 1652, 1130, 1040, 981, and 876 cm^{-1}, which are assigned to PO_4 and $HOPO_3$ stretching modes. O−P−O bending modes appear at 606, 564, and 523 cm^{-1}. The spectra of HAP prepared from solutions at an initial pH 8 show strong bands at 1652 and between 1105 and 1000 cm^{-1}. They are attributed to PO_4 and $HOPO_3$ stretching modes. The band at 870 cm^{-1} is ascribed to the P−(OH) stretching mode. In addition, HAP has two weak shoulders at 638 and 575 cm^{-1} and two bands of medium intensity at 603 and 563 cm^{-1}. These shoulders and bands are probably components of the PO_4 bending mode.

IR spectra of samples annealed at 85 °C (transformation to monetite) exhibit bands that are similar to brushite bands between 1652 to 500 cm^{-1}. The main difference between the spectra of the as-prepared and the annealed samples is that the −OH band at 3300 cm^{-1} is less intense after thermal treatment due to desorption of crystal water. This also qualitatively confirms XRD.

Scanning electron microscopy (SEM) of the samples grown at an initial pH 5 shows that control samples are identical to those reported earlier.[16] Similar to the control samples, samples grown with PEO-*b*-PLK form relatively thin plates extending over 50 μm in length. In contrast, samples grown with PEO-*b*-PLE contain smaller but rather thick and aggregated plate-like entities. They are between 5 and 10 μm long and 500 to 600 nm thick (Figure S3,

(38) Harada, A.; Cammas, S.; Kataoka, K. *Macromolecules* **1996**, *29*, 6183.
(39) Ryskin, Y. I.; Stavitskaya, G. P. *Opt. Spectrosc. (USSR), English Transl.* **1960**, *8*, 320.
(40) Herzberg, G. *Molecular Spectra and Molecular Structure; Infrared and Raman Spectra of Polyatomic Molecules*; van Nostrand: Princeton, 1954; Vol. II.
(41) Sivakumar, G. R.; Girija, E. K.; Narayana Kalkura, S.; Subramanian, C. *Cryst. Res. Technol.* **1998**, *33*, 197.

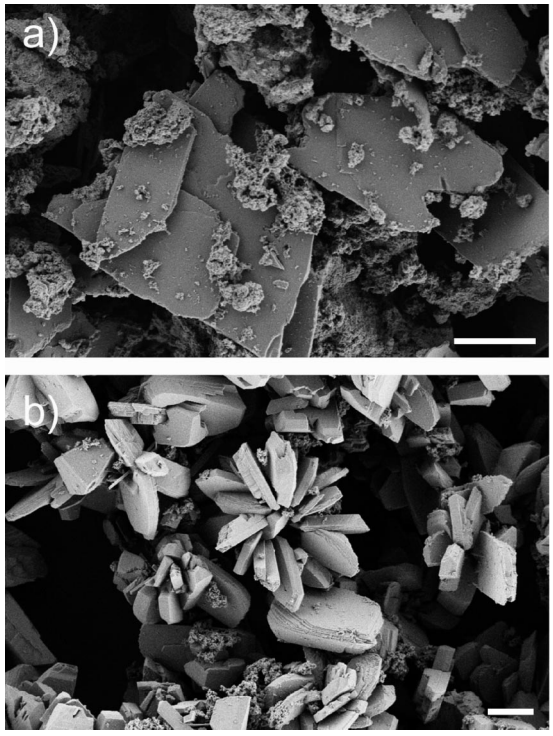

Figure 2. SEM images of (a) calcium phosphate obtained at pH 5 in the absence of polymer and annealed at 85 °C and (b) calcium phosphate obtained at pH 5 in the presence of PEO-*b*-PLE and annealed at 85 °C. Scale bars are 10 μm.

Supporting Information). Figure 2 shows that annealing at 85 °C has essentially no effect in the control sample and the samples precipitated with PEO-*b*-PLE.

Figure 3 shows that annealing of the samples grown with PEO-*b*-PLK leads to large crystals. They have a plate-like morphology and seem to contain many channel-like features running along the surface of the plate. Moreover, some much smaller, powder-like material is observed, similar to the smaller features observed in Figure 2a. The overall size of the large crystals is, similar to before the annealing, approximately 50 μm, and the thickness is approximately 75 nm. The channel-like features run parallel to the main faces of the plates, and side views of the crystals suggest that they not only are present on the particle surface but apparently run through the whole crystal. Moreover, SEM clearly shows that these channel-like features form domains where a number of them run roughly parallel to one another. The orientation of neighboring domains is not correlated, and there are numerous grain boundaries between the individual domains.

The channel-like features are between approximately 15 and 40 nm wide and up to approximately 2 μm long. Measurements at multiple positions along one feature show that there is some variation in the width of the features. However, there are no large width differences in the sense that all features are on the same order of magnitude (Figure 3d). A very rough estimate of the surface area σ from SEM gives $\sigma = 4\phi/(\rho T) \approx 6.8$ m^2/g, if the volume fraction of the pores $\phi = 15\%$, the mean chord length (pore diameter) $T =$ 30 nm, and the density of monetite $\rho \approx 2.93$ g/cm^3.[42] If one additionally assumes that only the monetite crystals (the large plate-like crystals) are porous, while the powder-like HAP

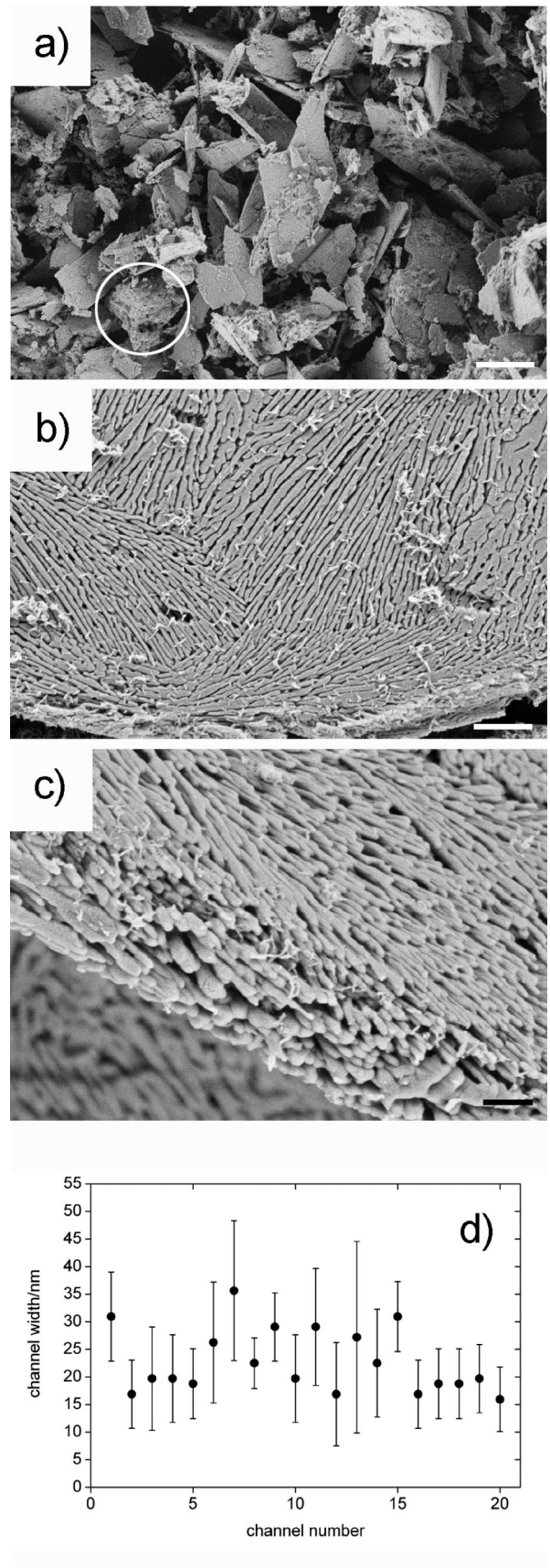

Figure 3. (a−c) SEM images of particles precipitated in the presence of PEO-*b*-PLK at an initial pH 5 after annealing at 85 °C. Scale bars are 30 μm (a), 1 μm (b), and 500 nm (c), respectively. (d) Average widths (10 measurements per channel) for 20 channel-like features in different crystals. Circle in panel (a) highlights the powdery material mentioned in the text.

is not, the total surface area reduces to approximately 3.4 m^2/g. This calculation is supported by porosity (BET) analysis, where a surface area of 2.5 m^2/g is determined.

Figure 4 shows TEM and electron diffraction data of a sample grown with PEO-*b*-PLK. Cross-sectional TEM shows that the plate-like crystals are indeed *not* large single-crystalline plates. Much rather, they are composed of smaller particles with sizes in the 100 nm range. This is similar to many earlier reports showing that calcium phosphate grows as approximately 100 nm needle-like particles.[19,43] Bright field TEM images also suggest that the small particles form domains, where the individual rods are roughly oriented parallel to each other. Unfortunately, it has not been possible to obtain electron diffraction data from individual domains because of their small size and instability toward the electron beam.

It has however been possible to obtain electron diffraction patterns from larger areas. These data suggest that the sample is polycrystalline, as there is no preferred orientation in the patterns. This suggests that, while there are small domains that are oriented, on a larger scale, there is no preferred orientation of the small particles within the large particles seen in the SEM.

As the electron beam leads to destruction of the crystals during electron diffraction experiments, we have used Raman microscopy to further clarify the phase assignments of the calcium phosphates. Figure 5a shows Raman spectra of the sample shown in Figures 3 and 4. Raman spectroscopy confirms our above hypothesis that the large, plate-like crystals consist of monetite because the bands at 903 and 986 cm^{-1} can be attributed to acid phosphate bands HPO_4^{2-} of monetite.[44] In contrast, the spectrum of the powder like material (circle in Figure 3a), which can also be observed in the sample, is attributed to hydroxyapatite with phosphate vibrations at 435, 592, 965, and 1052 cm^{-1}.[45,46]

In an attempt to more accurately determine the structure of the plates, we have also used synchrotron microcrystal diffraction on a single plate-like particle grown with PEO-*b*-PLK. This experiment confirms the presence of pure monetite and the absence of hydroxyapatite within this crystal type. Additionally, it was found that the crystal, even though it is not a perfect single crystal, is strongly textured (Figure 5b). Rotating the sample reveals more information about this texture. The (010) reflection appears as a sharp spot only when the plate is rotated by about +90° with respect to the plate normal, which indicates that the (010) crystallographic planes lie within the plane of the plate. Therefore, although it is difficult to image the orientation of the rods in the TEM, synchrotron X-ray diffraction provides clear evidence of a relatively highly correlated structure in each large crystal.

Finally, thermogravimetric (TGA) and differential thermal analysis (DTA) was done to assess the organic content and the phase transition at 85 °C (Figure S4, Supporting Information). The pure polymers are stable up to 100 °C. A weight loss of 5−6% in this region is attributed to water desorption. This is consistent with the endothermic heat flow

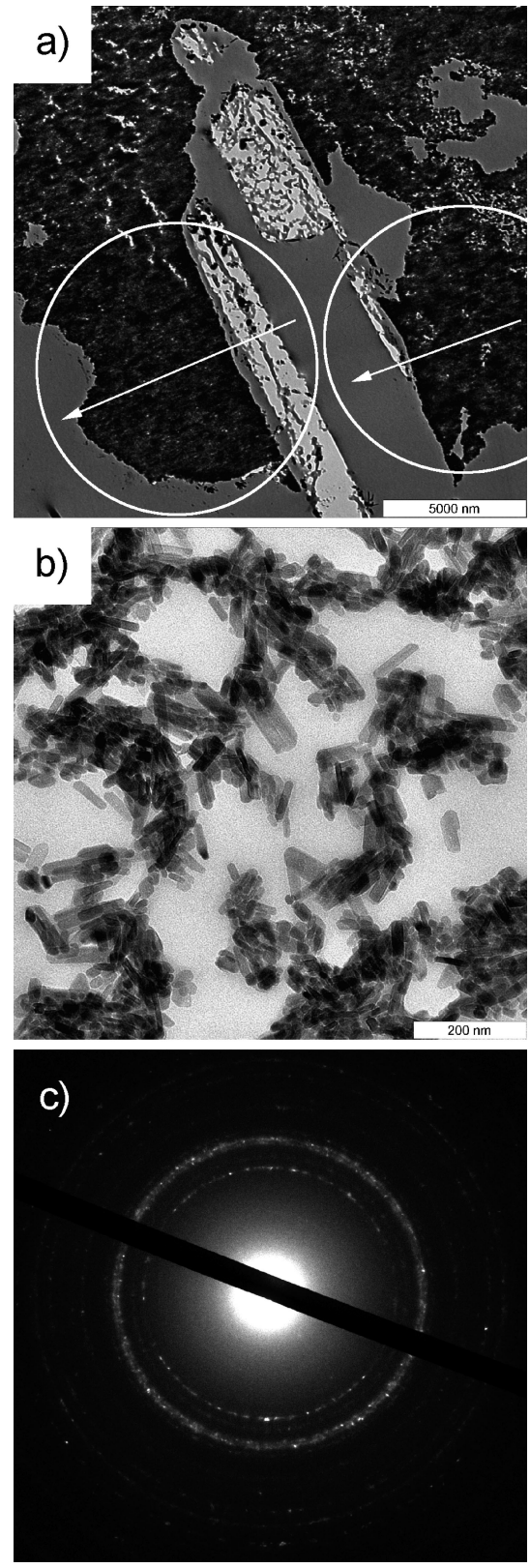

Figure 4. (a, b) Cross-sectional TEM image of the sample shown in Figure 3. Circles in (a) highlight areas with small particles of the same orientation. Arrow gives the general orientation of the long axis of the rods. (b) Higher magnification bright field image of nanometer-sized building blocks. (c) Selected area electron diffraction pattern of a larger region.

(42) Sapei, L.; Noeske, R.; Strauch, P.; Paris, O. *Chem. Mater.* **2008**, *20*, 2020.
(43) Furuichi, K.; Oaki, Y.; Imai, H. *Chem. Mater.* **2006**, *18*, 229.
(44) Casciani, F.; Condrate, R. A., Sr. *J. Solid State Chem.* **1980**, *34*, 385.
(45) Wilson, R. M.; Elliot, C. J.; Dowker, S. E. P.; Rodriguez-Lorenzo, L. M. *Biomaterials* **2005**, *26*, 1317.
(46) Walters, M. A.; Leung, Y. C.; Blumenthal, N. C.; LeGeroes, R. Z.; Konsker, K. A. *J. Inorg. Biochem.* **1990**, *39*, 193.

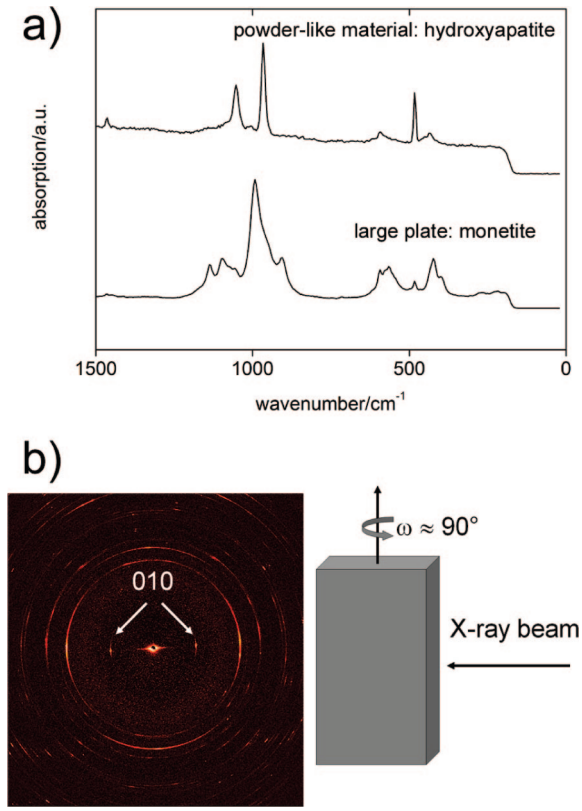

Figure 5. (a) Raman spectra of powder-like material and single plate. (b) X-ray pattern obtained via synchrotron microcrystal diffraction on a single plate-like crystal and schematic of the experiment.

in the DTA curve. The mass losses between 100 and 340 °C for PEO-*b*-PLK (60%) and between 170 and 380 °C for PEO-*b*-PLE (57%) and the exothermic DTA signal in this region are assigned to the partial oxidation, depolymerization, and condensation of the polymers. At temperatures above approximately 340−380 °C there is a final exothermic weight loss for both polymers, which is assigned to the final decomposition ("burning") of the polymers.

Upon heating, all precipitates show a similar behavior. A first minor weight loss (about 1%) below 200 °C is attributed to the evaporation of residual water, which is supported by the endothermic signal in the DTA. The second weight loss (ca. 13%) between 200 and 1000 °C in the samples precipitated with PEO-*b*-PLK is attributed to the oxidation and depolymerization of the organic material within the composite. This is supported by the observation of two exothermic peaks in DTA. The weight loss between 200 and 1000 °C (ca. 7%) in samples precipitated with PEO-*b*-PLE is more complex and shows several overlapping processes in DTA. It has been pointed out earlier that these processes are difficult to identify and separate[16] but that they can be assigned to the oxidation of polymer and the transformation of brushite and monetite to pyrophosphate. Overall, TGA/DTA suggests that the samples consist of about 90 wt % of calcium phosphate.

Discussion

In summary, our data show that the nature of the polyelectrolyte block (cationic or anionic) has a dramatic effect on the structure of the resulting precipitate. Only in the presence of a polycationic block, calcium phosphate with an intriguing channel-like morphology forms via a soft chemistry approach. However, the transition from brushite to monetite has been studied before. Monma et al.[47] have studied the hydrolysis of brushite (DCPD), monetite (DCPA), and α-TCP in basic aqueous solution at different temperatures. HAP prepared from DCPD consists of densely packed irregular rod-like crystals. Precipitates from α-TCP are porous aggregates of needle-like crystals, and precipitation from DCPA results in entangled long needle-like crystals.

Bigi et al.[18] have investigated the hydrolysis of octacalcium phosphate (OCP) to HAP in aqueous solution at pH 7.4 and different concentrations of poly(L-aspartate) and poly(L-glutamate). Without polyelectrolyte, the transformation of OCP into HAP is complete in 48 h. Both PLD and PLE inhibit OCP hydrolysis. However, PLE displays a greater inhibiting effect, which is shown by the different extent of phase transformation obtained at the same polyelectrolyte concentration. The inhibition takes place through polyelectrolyte adsorption on the (100) face of OCP crystals, which prevents the splitting of OCP crystals along their *c*-axis and the transformation into the final, very long, needle-like apatite crystals.

Bar-Yosef Ofir et al.[48] have studied the influence of PLE and PLK on the transformation kinetics of amorphous calcium phosphate (ACP) to crystalline phases in aqueous solution at pH 7.4. At low concentration (0.1 mM) both amino acids have an induction effect on crystallization, but the effective concentration region is one order of magnitude smaller for PLE (0.3−0.4 mM) than for PLK (4 mM). In contrast, at high concentrations the amino acids are inhibitors and the inhibition efficiency of crystallization for PLE is about 20 times stronger than for PLK.

Finally, Furuichi et al.[42] reported the preparation of nanostructured apatite networks via basic hydrolysis of dicalcium phosphate (DCPA, monetite) obtained by the dehydration of DCPD precipitated in gelatin. The DCPA crystals also have a rod-like morphology. The authors claim that specific interactions of the gelatin molecule with the calcium phosphate crystals play a key role in this transition. The authors also claim that the gelatin present in the crystals facilitates the dehydration process such that long rod-like crystals form.

In our case, annealing of the samples at 85 °C triggers desorption of water and transformation of the precipitates into monetite. This phase transition takes place at approximately 60 °C and has been observed before.[40] While it is not clear yet where the polymers are located in our crystals, it is obvious that the change from a polyanionic block to a polycationic block has both an influence on the phase selection during crystal growth and also on the dehydration process upon annealing. The study therefore shows that polycations are useful and interesting, yet poorly explored, crystallization additives for the precipitation of calcium phosphate.

(47) Monma, H.; Kamiya, T. *J. Mater. Sci.* **1987**, *22*, 4247.
(48) Bar-Yosef Ofir, P.; Govrin-Lippman, R.; Garti, N.; Füredi-Milhofer, H. *Cryst. Growth Des.* **2004**, *4*, 177.

Overall, SEM, TEM, XRD, IR, and Raman spectroscopy suggest that the large particles, which at first glance seem to be single crystalline particles containing (surface) channels, are in fact large crystals built from approximately 100-nm-sized acicular or rod-like subunits. The micrometer-sized plate-like shape of the as-synthesized large crystals, which crystallographically is brushite, could then arise from the fact that the individual brushite needles aggregate and ultimately replicate the well-known brushite plate morphology. A high correlation of the nanoscale needles even after annealing is indeed confirmed by the synchrotron experiment, where a highly textured material was found, Figure 5.

In contrast, TEM and electron diffraction (Figure 4) seem to suggest that the correlation is somewhat lower, as especially electron diffraction shows patterns characteristic of polycrystalline order. We explain this discrepancy with sample preparation. Presumably, the crystals were disrupted during microtomy prior to TEM experiments, leading to the observed lower order. In contrast, the synchrotron measurements were made on an as-synthesized and annealed crystal without further sample preparation other than mounting on a needle. As a result, synchrotron X-ray diffraction likely exerts much less external force and thus structural changes on the crystal than microtomy.

Possibly, the polymer has an additional orientation effect, for example, by polymer/phosphate interactions similar to those reported by Lutz et al.[24] However, as brushite grown in the absence of the polymer shows the same morphology,[16,49] this cannot be unambiguously ruled in or out. Finally, it must also be noted that the formation of the channel-like features has at the moment not been observed with all polycations investigated in the laboratory. For example, poly(ethylene oxide)-*block*-poly(ethylene imine) di- and triblock copolymers do not show this effect. This observation suggests that there is more to the formation of the channel-like features than simply a number of positive charges.

(49) Tang, R.; Darragh, M.; Orme, C. A.; Guan, X.; Hoyer, J. R.; Nancollas, G. H. *Angew. Chem. Int. Ed.* **2005**, *44*, 3698.

Conclusion

Polycationic polymers have relatively rarely been studied in the context of bioinspired mineralization. The current paper shows that, in some cases, polycations can add value to biomimetic mineralization processes. The channel-like features observed in the current study only form with polycationic additives followed by a mild heat treatment. As a result, our previous[16,25] and current data introduce polycations as valuable mineralization additives for advanced, nanostructured organic/inorganic composite materials.

Acknowledgment. We thank R. Rothe for BET measurements, Dr. A. Friedrich for TGA measurements, Dr. B. Tiersch, H. Runge, and R. Pitschke for SEM measurements, and Dr. B. Aichmayer, S. Siegel, and C. Li for help with synchrotron microbeam diffraction experiments. A.S. acknowledges the MPI of Colloids and Interfaces for a postdoctoral fellowship. H.S. acknowledges Erich C. We thank the MPI of Colloids and Interfaces (Colloid Chemistry), the University of Potsdam, and the Fonds der Chemischen Industrie for financial support. A.M. thanks the Adolf-Martens-Fonds e.V. for an Adolf-Martens-fellowship.

Supporting Information Available: Scanning electron micrographs, thermogravimetric analysis data, and SEC data (PDF). This material is available free of charge via the Internet at http://pubs.acs.org.

CM803244Z